Journal Pre-proof

Recent progress in the synthesis of lanthanide-based persistent luminescence nanoparticles

Yurong Wei, Chengxu Gong, Min Zhao, Lei Zhang, Shaodan Yang, Peixu Li, Zhao Ding, Quan Yuan, Yanbing Yang

Please cite this article as: Wei Y, Gong C, Zhao M, Zhang L, Yang S, Li P, Ding Z, Yuan Q, Yang Y, Recent progress in the synthesis of lanthanide-based persistent luminescence nanoparticles, *Journal of Rare Earths*, https://doi.org/10.1016/j.jre.2022.05.016.

This is a PDF file of an article that has undergone enhancements after acceptance, such as the addition of a cover page and metadata, and formatting for readability, but it is not yet the definitive version of record. This version will undergo additional copyediting, typesetting and review before it is published in its final form, but we are providing this version to give early visibility of the article. Please note that, during the production process, errors may be discovered which could affect the content, and all legal disclaimers that apply to the journal pertain.

Thermal
decomposition

Template

Sol-gel

Ln-based persistent
luminescence NPs

Hydrothermal
reaction

Microwave-assisted
synthesis

Co-precipitation

Recent progress in the synthesis of lanthanide-based persistent luminescence nanoparticles

Yurong Wei[a,†], Chengxu Gong[a,†], Min Zhao[a], Lei Zhang[b], Shaodan Yang[c], Peixu Li[c], Zhao Ding[a,*], Quan Yuan[b], Yanbing Yang[a,*]

[a]College of Chemistry and Molecular Sciences, School of Microelectronics, Department of Colorectal and Anal Surgery, Hubei Key Laboratory of Intestinal and Colorectal Diseases, Zhongnan Hospital of Wuhan University, Wuhan University, Wuhan 430072, China

[b]Molecular Science and Biomedicine Laboratory (MBL), State Key Laboratory of Chemo/Biosensing and Chemometrics, College of Chemistry and Chemical Engineering, Hunan University, Changsha 410082, China

[c]Luoyang Advanced Manufacturing Industry R&D Center, Tianjin Research Institute for Advanced Equipment, Tsinghua University, Luoyang 471003, China

[†]These authors contributed equally to this work.

ABSTRACT:

Persistent luminescence nanoparticles (PLNPs) are a kind of phosphors that can remain luminescent for seconds to several days after the stoppage of excitation. Lanthanides show the special capability to largely broaden the emission range and enhance the luminescence intensity of PLNPs due to their dense energy structure and unique electronic configurations. In the past decades, various methods have been developed for the synthesis of lanthanide-based PLNPs with excellent persistent luminescence properties, and the lanthanide-based PLNPs are widely studied in areas including biomedicine, energy, and information storage. In this review, we summarize the research progress in the synthesis of lanthanide-based PLNPs and outlined several typical synthesis methods. We discuss the fundamental concepts of preparation methods as well as the advantages and drawbacks of the typical synthetic approaches. Moreover, the current challenges and the potential solutions for the development of lanthanide-based PLNPs are also discussed in an attempt to provide strategies to further improve the optical properties of lanthanide-based PLNPs. We hope this review can contribute to the design of lanthanide-based PLNPs with desired properties and further promote their applications in biomedicine, energy, and information science.

Keywords: lanthanide; persistent luminescence; nanoparticles; defects; bioimaging; rare earths

* Corresponding author: College of Chemistry and Molecular Sciences, School of Microelectronics, Department of Colorectal and Anal Surgery, Hubei Key Laboratory of Intestinal and Colorectal Diseases, Zhongnan Hospital of Wuhan University, Wuhan University, Wuhan 430072, China

* E-mail addresses: yangyanbing@whu.edu.cn (YB. Yang), dingzhao@whu.edu.cn (Z. Ding).

Tel: +86 027-68756362

1. Introduction

Persistent luminescence is a phenomenon whereby luminescence can remain for a few seconds to several days after the excitation ceases, leading to the well-known glow-in-the-dark phenomenon. For example, the legendary luminous pearl in ancient China can emit bright persistent luminescence at night. In 1996, Matsuzawa developed the proverbial $SrAl_2O_4:Eu^{2+},Dy^{3+}$ phosphor that displays a bright green persistent luminescence with decay time over 30 h after the cessation of UV light excitation.[1] The persistent luminescence intensity of $SrAl_2O_4:Eu^{2+},Dy^{3+}$ was 10 times stronger than that of the commercially available $ZnS:Cu^{2+},Co^{2+}$ persistent phosphor at the time. From then on, persistent luminescence has received massive attention. A great variety of persistent phosphors have been developed and persistent phosphors are widely used in areas such as emergency signage, luminous coatings, and defense.[2] In the past years, the application potential of PLNPs has been extended to biomedicine. Persistent luminescence nanoparticles show unique advantages in biomedicine owing to their potent ability in eliminating autofluorescence interference and tissue scattering interference. Additionally, PLNPs are suitable for long-term bioimaging and bio-tracing due to their long-live luminescence. Many biosensing and bioimaging strategies with ultra-high signal-to-noise ratio and sensitivity have been developed based on the virtues of PLNPs.[3–6] Beyond biomedicine, PLNPs have also been applied in photocatalysis, solar cells, and information storage or encryption.[7] The virtues of PLNPs in different research areas remain to be explored in the future.

In the past five decades, lanthanide ions have been largely used to develop persistent phosphors with bright and durable persistent luminescence at different emission regions. Lanthanide ions possess ladder-like dense energy structures and they can produce narrow emissions ranging from UV to NIR-II region, which makes lanthanide ions the ideal emission center in phosphors.[8–13] Moreover, lanthanide ions display similar charges and radii, suggesting that the doped lanthanide ion can be easily replaced by another one to realize significantly different emission wavelengths or intensities.[8] An unprecedented advantage of lanthanide-doped persistent phosphors is the generation of strong persistent luminescence in the NIR region, particularly the NIR-II region. The NIR region falls into biological optical transparency windows ranging from NIR-I (650–950 nm), NIR-II (1000–1350 nm), to NIR-III (1500–1800 nm).[3] At the very beginning, persistent luminescence was restricted to the UV-visible region until the expansion of using the lanthanide ions. With the rapid development of lanthanide-doped persistent phosphors, many researchers have reported the NIR persistent emission based on lanthanide doping. In a word, lanthanide ions are beneficial to broaden the emission range, strengthen the luminescence intensity and prolong the decay time of persistent phosphors. In the past years, the lanthanide-doped persistent phosphors are in rapid development and many newly emerged lanthanide-based PLNPs with unexplored applications have been reported.[14–16] Several reviews focusing on persistent phosphors and their applications have been presented.[3–7] However, seldom reviews have focused on the synthesis methods of lanthanide-based PLNPs.

Our group concentrated on the synthesis, surface modification, and biomedical applications of PLNPs.[3,17–21] Since the properties and applications of PLNPs are highly correlated with the synthesis protocols, this review aims to introduce the latest progress in the design and synthesis of lanthanide-based PLNPs. The typical PLNPs synthesis methods were summarized. The merits and drawbacks of the corresponding synthetic approaches were comprehensively reviewed. Also, the prospects and challenges in the controlled synthesis of lanthanide-based PLNPs were discussed.

We hope this review can offer instructions for the preparation of lanthanide-based PLNPs and further promote the applications of lanthanide-based PNLPs in biomedicine, energy, and information science.

2. The persistent luminescence mechanism of lanthanide-doped PLNPs

Figure 1. Lanthanide-based persistent luminescence phosphors with different emission wavelengths. Reprinted with permission from Ref. 2. Copyright 2018 Elsevier.

Lanthanide-based persistent phosphors are usually composed of inorganic matrixes (known as hosts) and activator Ln^{3+} ions such as Eu^{2+}, Dy^{3+}, Tb^{3+}, Sm^{3+}, Nd^{3+}, and Sm^{3+}. The matrixes can be sulfides, alkaline earth aluminates, oxides, silicates, etc. (Fig. 1).[2] The inorganic matrixes can provide a special crystal field to influence the energy levels of lanthanide ions, and the doping of the same lanthanide ions into different matrixes can easily produce significantly different persistent luminescence properties. Since the emergence of $SrAl_2O_4:Eu^{2+},Dy^{3+}$, many kinds of lanthanide-doped $SrAl_2O_4$ persistent phosphors have been developed, as listed in Table 1.[22–32] Among all the lanthanide ions, Eu^{2+} is the most common luminescence center in lanthanide-doped PLNPs (Table 2).[33–43] The strong crystal field of Eu^{2+} decreases the minimum emission level and results in tunable yellow, orange and red emissions, leading to the development of a large amount of Eu^{2+}-doped persistent phosphors.[44–46] The general mechanism of persistent luminescence is illustrated in Fig. 2. Under UV excitation, the electrons in the valence band (VB) of lanthanide-doped persistent phosphors are pumped to the conduction band (CB). The abundant excited states of lanthanide ions that are close to the conduction band minimum (CBM), such as the 5d levels, can accept electrons from the CBM and further generate photoluminescence. Moreover, part of the excited electrons can be trapped by crystal defects in the persistent phosphors. After excitation ceases, the trapped electrons can be slowly thermally stimulated and further transferred to the excited states of lanthanide ions, leading to the generation of persistent luminescence.[47]

Table 1 Summary of lanthanide-based persistent phosphors of $SrAl_2O_4$. The decay time is defined as the time when the luminance has decreased to 0.32 mcd/m^2.[48]

Host	Dopants	$\lambda_{emission}$	Decay time	Synthesis method	References
$SrAl_2O_4$	Eu^{2+},Dy^{3+},Tb^{3+}	513 nm	2743 s	Combustion	22
	Eu^{2+},B^{3+},Dy^{3+}	508 nm	>120 min	Solid-state reaction	23
	$Eu^{2+},(Ln)\ Ce^{3+},\ Pr^{3+},Tb^{3+}$	380 nm	—	Combustion	24
	Ho^{3+},Yb^{3+},Li^+	556 nm, 664 nm	—	Solid-state reaction	25
	Eu^{2+},Yb^{3+}	519 nm, 978 nm	—	Hydrothermal method	26
	Eu^{2+},Dy^{3+}	520 nm	30 h	Solid-state reaction	1
	Eu^{2+},Dy^{3+}	516 nm	16 h	Hydrothermal method	27
	Eu^{2+},Dy^{3+}	517 nm	>1500 s	Combustion	28
	Eu^{2+},Er^{3+},Dy^{3+}	525 nm, 649 nm, 1530 nm	>10 min	Combustion	29
	Ce^{3+}	385 nm	>10 h	Solid-state reaction	30
	Eu^{2+}	513 nm	5 s	Solid-state reaction	31
	Eu^{2+},Cr^{3+}	515 nm, 760 nm	1000 s	Sol-gel-combustion	32

Table 2 Known Eu^{2+}-activated persistent phosphors.

Host	Dopants	$\lambda_{emission}$	Decay time	Synthesis method	References
$(Sr,Ca,Ba)Al_2O_4$	Eu^{2+},Dy^{3+}	520 nm to 500 nm	1088.5 ms - 219.91 ms	Solid-state reaction	33
$Ca_4(PO_4)_2O$	Eu^{2+},Y^{3+}	690 nm	2 h	Solid-state reaction	34
$ZnAl_2O_4$	Eu^{2+},Eu^{3+}	615 nm	—	Sol-gel synthesis	35
$CdSiO_3$	Mn^{2+},Eu^{2+}	587 nm	>5 h	Sol-gel synthesis	36
$BaMg_2(PO_4)_2$	Eu^{2+},Ln^{3+} (Ln=Ce, Pr, Tb and Lu)	435 nm, 543 nm	—	Solid-state reaction	37
$CaAl_2O_4$	$Eu^{3+}/Eu^{2+},Nd^{3+}$	450 nm	2 h	Combustion	38
$Sr_3Al_2O_6$	Eu^{2+},Dy^{3+}	612 nm	20 min	Sol-gel-microwave	39
Zn_2GeO_4	Eu^{2+}	474 nm	198 s	Solid-state reaction	40
$CaMgSi_2O_6$	Eu^{2+},Mn^{2+},Pr^{3+}	685 nm	900 s	Sol-gel synthesis	41
CaS	Eu^{2+},Dy^{3+}	650 nm	5 h	Co-precipitation	42
Sr_3SiO_5	Eu^{2+}	580 nm	7000 s	Co-precipitation combined with solid-state reaction	43

Figure 2. Simplified persistent luminescence mechanism. Reprinted with permission from Ref. 46. Copyright 2019 Royal Society of Chemistry.

3. Synthesis of lanthanide-based PLNPs

Many methods have been developed for the synthesis of lanthanide-based PLNPs and each method has its merits and limitations. The solid-state reaction is the conventional synthesis method of lanthanide-based persistent phosphors and it involves the mixing of precursors and high-temperature annealing treatment.[1] The advantages of the solid-state reaction include simplicity and the tendency to produce crystal defects at high calcination temperatures.[49–52] The produced crystal defects can trap the charge carriers during excitation, which leads to the generation or enhancement of persistent luminescence. However, the lanthanide-based persistent phosphors synthesized by the solid-state reaction are often blocky materials with large size, poor dispersibility and surface functionalization.[53–59] The biomedical applications require persistent phosphors to have small sizes, good dispersity and easy modification. To prepare lanthanide-based PLNPs with nano size and strong persistent luminescence, various methods have been developed, such as the sol-gel method, hydrothermal method, thermal decomposition method, co-precipitation method, template method and microwave-assisted method. We have summarized the basic synthesis principles of the synthesis methods for lanthanide-based PLNPs and evaluated their merits and limitations. A simple comparison of these methods including processing conditions, advantages and disadvantages is listed in Table 3.

Table 3. Comparison of typical synthesis approaches for lanthanide-based PLNPs.

Synthesis methods	Specified temperature	Reaction time	Advantages	Disadvantages
Sol-gel	Low ($\leqslant 80\ °C$)	$\leqslant 24$ h	Uniform morphology, good	Long reaction time,

			Luminescent properties, high productivity, great crystallinity	Broad size distribution, agglomerated products, produce a large amount of gas
Hydrothermal	Moderate ($\leqslant 300$ °C)	10–24 h	Tunable size and morphology, cost efficient, great crystallinity	Long reaction time, high pressure, excellent luminescent properties
Thermal decomposition	Moderate to high (100-800 °C)	long reaction time	High homogeneity and purity, good luminescent properties, great crystallinity	Expensive set up, toxic by product, low product yield
Co-precipitation	Relatively low ($\geqslant 150$ °C)	20 min to 24 h	Uniform size and morphology, low cost, nontoxic reagent	Long reaction time, poor crystallinity, poor luminescent properties
Template	Low ($\leqslant 100$ °C)	3–10 h	Simple operation, regular spherical morphologies, uniform size and morphology	Poor luminescent properties, poor crystallinity, limited by templates
Microwave	Low ($\leqslant 150$ °C)	$\leqslant 20$ min	High productivity, fast, safe, and economic	Poor luminescent properties, poor crystallinity

3.1. Sol-gel method

The sol-gel process is a wet-chemical technique that is widely used to synthesize nanoparticles. Compared to other wet chemical techniques, sol-gel is a well-established method and shows particular advantages in obtaining materials from chemically homogeneous precursors.[60–65] By controlling the state of the solution, the materials can be synthesized rapidly at a low temperature with an atomic-level mixing of reagents. Furthermore, the size, morphology and properties of the particles can be precisely controlled in the sol-gel reactions.[66–68]

Figure 3. (a) Time-dependent persistent luminescence spectra of $Zn_{2.94}Ga_{1.96}Ge_2O_{10}$:$Cr^{3+}$,$Pr^{3+}$ PLNPs; TEM (b) and high-resolution TEM (c) images of the PLNPs; (d, e) The persistent luminescence decay curves of $Zn_zGa_{1.96}Ge_2O_{10}$:$Cr_{0.01}Pr_{0.03}$ and $Zn_3Ga_{2-x-y}Ge_2O_{10}$:Cr_xPr_y; (f) Persistent luminescence decay curve of the PLNPs. Reprinted with permission from Ref. 75. Copyright 2013 American Chemical Society.

The main processes of sol-gel methods can be simply described in four steps: (1) synthesis of "sol" through hydrolysis and condensation of molecular precursors, (2) formation of gel *via* polycondensation, (3) suspending and drying the particles, and (4) annealing the products. The precursors used in the sol-gel synthesis reaction are generally metal salts or alkoxides. The suitability of metal salts or alkoxides for the sol-gel method lies in several factors, including the

electronegativity difference between the metal and oxygen, and the electronic effect of the alkyl/aryl chain on the stability of the alkoxy groups. Both of these two factors can affect the relative rates of hydrolysis and condensation, ultimately conducting gel structure through the degree of polymerization or oligomerization. Many other factors can also impact the rates of hydrolysis and condensation, such as solvents, acid or base catalysts, the ratio of water to alkoxide and the presence of chelating agents.[69]

The sol-gel method has been largely used in the preparation of lanthanide-based PLNPs.[41,70–73] Teixeira et al. prepared $Eu^{3+},Ti^{3+}/Ti^{4+}$ co-doped Y_2O_3 PLNPs by utilizing the coconut water-assisted sol-gel method and obtained nanoparticles with sizes in the range of 30–100 nm.[74] Yan et al. synthesized NIR-emitting $Zn_{2.94}Ga_{1.96}Ge_2O_{10}:Cr^{3+},Pr^{3+}$ PLNPs with a persistent luminescence decay time of more than 15 d by a citrate sol-gel method. They showed that the co-doping of lanthanide Pr^{3+} can produce suitable Zn deficiency in host lattice and further led to the prominently enhanced persistent luminescence in the $Zn_{2.94}Ga_{1.96}Ge_2O_{10}:Cr^{3+},Pr^{3+}$ PLNP. The PLNPs were promising for the long-term *in vivo* targeted tumor imaging after surface functionalization with PEG and c(RGDyk) peptide (Fig. 3).[75] The controllability with various factors makes the sol-gel method an easy-performed method to produce PLNPs with narrow size distributions, high crystallinity and uniform morphology.

3.2. Hydrothermal method

The hydrothermal method refers to allowing the precursors to react under high temperature and high pressure in a sealed environment such as an autoclave or flow reactor.[76–83] With the system heated up and pressure rising, the precipitation occurs at the surface of the liquid phase as the solutions are perturbed. The nanoparticles are separated from the reaction solution through centrifuging and subsequent high-temperature annealing treatment is optional to increase the crystallinity of the nanoparticles. The properties of the nanoparticles can be easily regulated by changing the reaction parameters like annealing temperature, reaction time, pressure and pH values. The preparation of PLNPs by the hydrothermal method was realized by many researchers. Liu et al. synthesized Cr^{3+} and Er^{3+} co-doped zinc gallogermanate ($ZGGO:Cr^{3+},Er^{3+}$) PLNPs with an average size of 60 nm using a similar hydrothermal method. The co-doping of Er^{3+} realized the NIR-III (~1540 nm) persistent luminescence due to the energy transfer from Cr^{3+} to Er^{3+}. Local-tissue NIR persistent luminescence imaging can be easily obtained by single-step 980 nm radiation.[84] Furthermore, they showed that an X-ray pre-irradiation followed by 980 nm light re-activation of the $ZGGO:Cr^{3+},Er^{3+}$ PLNPs was promising to produce strong and durable NIR persistent luminescence, making the $ZGGO:Cr^{3+},Er^{3+}$ PLNPs valuable in deep-tissue bioimaging. These studies show that the hydrothermal method is promising in the synthesis of lanthanide-based PLNPs with uniform size and easy surface functionalization. However, this method suffers from high-temperature reactions, a long reaction time, and low product yield.

Figure 4. Afterglow decay curves of the $ZGGO:Cr_x^{3+},Er_y^{3+}$ ($x = 0$ and 0.02; $y = 0$, 0.01, 0.02, 0.03, and 0.04) monitored at 1540 nm (a) and 696 nm (b); (c) Emission spectra of the $ZGGO:Cr_x^{3+},Er_y^{3+}$ ($x = 0$ and 0.02; $y = 0$, 0.01, 0.02, 0.03, and 0.04) afterglow nanoparticles; (d) Afterglow mechanisms after cessation of X-ray and/or NIR light irradiations based on the energy transfers between Cr^{3+} and Er^{3+}. Reprinted with permission from Ref. 84. Copyright 2021 John Wiley and Sons.

3.3. Thermal decomposition method

Despite high-temperature thermal decomposition being a young synthesis method for nanomaterials, there are a large number of lanthanide-based PLNPs with excellent properties prepared by this method. Miletto et al. have synthesized a series of hexagonal II-Type lanthanide-based $Gd_{2-x}RE_xO_2CO_3$ (RE^{3+}= Eu^{3+}, Yb^{3+}, Dy^{3+}) PLNPs by thermal decomposition method. They showed that Yb^{3+} doped Gd-oxycarbonate displayed especially promising in biomedicine due to its strong NIR persistent luminescence.[85] Recently, Liu et al. prepared $NaGdF_4$:Yb/Tm@$NaGdF_4$:Ce/Mn@$NaYF_4$ multilayer PLNPs with a long-lived green emission.[86] In a typical synthesis protocol, the lanthanide precursors are mixed with oleic acid (OA), oleylamine (OM), and 1-octadacane (ODE). OA and OM can decrease the aggregation of PLNPs and further control the growth of nanoparticles, while ODE offers a high-temperature decomposition environment. The thermal decomposition system is heated under high temperatures (usually above 300 °C) and the precursors decompose to form the PLNPs. Owing to its relatively high-temperature treatment, the obtained lanthanide-based PLNPs usually have long persistent luminescence. Recently, Zhang et al. synthesized a series of X-ray-activated, lanthanide-based $NaY(Gd)F_4$ PLNPs with an extremely long decay time of more than 45 d in the NIR-II region *via* the thermal decomposition method. The prepared lanthanide-based PLNPs have a tunable NIR-II persistent luminescence due to their core-shell structure. The PLNPs were applied in tumor imaging and the T/N ratio is up to quadruple higher than that of NIR-II fluorescence in signal-to-noise ratios. With the characteristics of tunable NIR-II persistent luminescence, nimble construction, controllable nanostructure and core-shell structure, the prepared lanthanide-based PLNPs have better encoding capacity, multilevel information encryption, higher contrast and resolution in deep tissue imaging.[87] Han et al. have also developed a series of core−shell CaF_2:Dy@$NaREF_4$ PLNPs with various morphologies *via* the thermal decomposition method and found the CaF_2:Dy@$NaYF_4$ possessed enhanced persistent luminescence under both light and X-ray excitations.[88] The thermal decomposition method could produce lanthanide-based PLNPs with high homogeneity, high crystallinity and narrow size distribution. Also, the synthesis process offers the possibility to synthesize ultra-small PLNPs with predefined optical properties for biomedical applications compared with the sol-gel or co-precipitation method.[89] As a burgeoning method, the high-temperature thermal decomposition method has proved its irreplaceable value in the preparation of lanthanide-based PLNPs.

Figure 5. Thermal decomposition synthesis of CaF_2:Dy@$NaREF_4$ core-shell PLNPs with various morphologies. TEM of CaF_2:Dy@$NaYF_4$:Ca (a), CaF_2:Dy@$NaGdF_4$ (b), CaF_2:Dy@$NaYbF_4$ (c) and CaF_2:Dy@$LiYF_4$ (d) core-shell PLNPs. Reprinted with permission from Ref. 88. Copyright 2021 American Chemical Society.

3.4. Co-precipitation method

Co-precipitation is a simple method to obtain nanoparticles by adding the precipitant agent into the saturated solution of soluble precursors, usually metal precursors. This method relies on the solubility and compatibility of original materials since it involves simultaneous precipitation of precursors in solution.[90–98] The mixed precursor forms an unstable supersaturated solution in which the solid atoms aggregate into small nuclei. The small nuclei spontaneously grow into

crystals and primary products, followed by the aggregation of the primary particles into larger nanoparticles. Generally, alkaline compounds are used as precipitant agents, such as urea, sodium bicarbonate, sodium silicate and EDTA. Taking urea as an example, the soluble metals and urea are hydrolyzed to generate metal hydroxides and ammonia. The pH of the solution raises as the hydrolysis continues, which gives rise to the precipitation of metal hydroxides and the formation of nanoparticles. Commonly, the properties of nanoparticles can be regulated by lots of parameters like the concentration of precipitant agents, metal precursors, the temperature of co-precipitation and the complexing agent.

Recently, Liu et al. have prepared a series of lanthanide-based $NaLuF_4:Tb@NaYF_4$ PLNPs with decay times of more than 30 d. They demonstrated an ultralong-lived X-ray trapping for flat-panel-free, high-resolution, three-dimensional imaging based on the prepared nanoparticles. They named this method X-ray luminescence extension imaging (Xr-LEI) due to its unprecedented characteristic to carry out radiography on highly curved 3D objects. They further studied the mechanisms of X-ray energy conversion through durable electron trapping and drew attention to the research in patient-centered radiography and imaging-guided therapeutics.[16]

3.5. Template method

The template method is also widely used to prepare different sorts of PLNPs.[99–105] Generally, a mixed ionic solution containing templates (usually mesoporous materials) is used as precursors. The impregnated templates are separated from the solution and dried, followed by annealing at a high temperature to produce nanoparticles with a narrow size distribution. Mesoporous silica nanospheres (MSNs) are the most commonly used template for the preparation of PLNPs. Chen et al. have prepared X-ray-charged, monodisperse porous zinc gallogermanates $Zn_3Ga_2GeO_8:Cr^{3+},Yb^{3+},Er^{3+}$ (mZGGOs) PLNPs with a uniform size distribution. These PLNPs are suitable for X-ray-induced bioimaging and photodynamic therapy, which can availably hinder the growth of orthotopic hepatic tumors (Fig. 4).[106] Recently, Wang et al. have designed a large-pore MSN-templated strategy to prepare multifunctional hybrid mesoporous PLNPs nanoparticles (HMNPs) which integrated the NIR-persistent luminescence nanoparticles ($Ga_2O_3:Cr^{3+},Nd^{3+}$), magnetic nanoparticles (Ga_2O_3) and radionuclides (^{68}Ga). The HMNPs inherited the structure of large-pore MSN templates and possessed superb drug loading capacity. The DOX/Si-Pc-loaded HMNPs exhibited excellent tumor suppression ability, suggesting the potential of the HMNPs in multimodal imaging-guided chemotherapy and photodynamic therapy.[107]

Figure 6. TEM image (a), high-resolution TEM image (b), nitrogen adsorption-desorption isotherms (c), and STEM-elemental mapping (d) of the mZGGOs PLNPs; (e) XRD patterns of ZGGO, $mSiO_2$, and mZGGOs. Reprinted with permission from Ref. 106. Copyright 2020 John Wiley and Sons.

3.6. Microwave-assisted method

Microwave is a fast and efficient method in the synthesis of lanthanide-based PLNPs. Recently, microwave-assisted solid-state and sol-gel synthesis strategies have gained enormous attention from researchers. In the case of microwave irradiation, the precursor solutions are heated homogeneously to promote the uniform nucleation and growth of nanoparticles. The obtained particles are roughly identical compared to the products synthesized without microwave

assistance.[108–110] Hermi et al. synthesized $Lu_2O_3:R^{3+}$,M (Pr, Hf; Eu; or Tb, Ca^{2+}) PLNPs via the microwave-assisted solid-state method with less than 7% reaction time compared to solution synthesis methods. The $Lu_2O_3:R^{3+}$,M PLNPs prepared by this method showed strong persistent luminescence with decay time ranging from 1100 s to 8 h after the UV excitation ceases. Besides, the adjustability of persistent luminescence offers the $Lu_2O_3:R^{3+}$,M PLNPs promising applications in both solar cells and bioimaging.[111] Due to the uniform and rapid heating of precursor solutions by microwave irradiation, microwave assistance can accelerate nucleation and crystal growth, significantly shortening the reaction time. For instance, Suresh et al. have prepared red-emitting near-spherical $ZnGa_{2-x}Eu_xO_4$ in just 10 min with microwave assistance.[112] The microwave-assisted method is regarded as an appropriate way for the rapid synthesis of lanthanide-based PLNPs.

3.7. Other methods

Except for the above-mentioned methods, other methods such as the combustion method, [23,113–118] salt microemulsion method,[119] molten salt-assisted method,[120] electrospinning method,[121,122] solvothermal method[123,124] and laser ablation techniques[125–128] are also capable of preparing lanthanide-based PLNPs. Combustion is a rapid and easy process that makes full use of the exothermic reaction between metal nitrates and organic fuels (including urea, carbohydrazide or glycine). The energy generated by the combustion of organic dyes could maintain a high temperature (up to 1000 °C) for more than 60 s to enable the crystalization and growth of PLNPs. Huczko et al. have used the combustion method to synthesize a series of $Y_3Al_5O_{12}:Ce^{3+}$ PLNPs with a size less than 100 nm under the temperature of 900 °C.[129] The rapidly produced high temperature by combustion can improve the energy storage ability of PLNPs due to the increased concentration of defects in the host lattice, as evidenced by the green-emitting $SrAl_4O_7:Eu^{2+},Ln^{3+}$ ($Ln^{3+}= Dy^{3+}, Pr^{3+}$ and Y^{3+}) synthesized by Brito et al.[130] However, the combustion method still has the disadvantages such as the lack of reproducibility and the uncontrollability of the process owing to the unpredictability of combustion, which usually leads to a broad range of particle size. Electrospinning is a well-established method in the preparation of one-dimensional nano/micro-fibers. Many PLNPs-embedded nano/micro-fibers with excellent mechanical toughness and large diameter to length ratio have been prepared with electrospinning technique. However, the fixed one-dimensional morphology makes it difficult for the electrospinning to become a universal or commercial method for the preparation of PLNPs with controllable properties. The laser ablation technique is an environment-friendly method for the preparation of PLNPs since it could obtain PLNPs in a fast and clean manner. Regardless, more effort is still required to improve the persistent luminescence properties, purity and morphology of the products obtained with the laser ablation technique.

4. Discussion and prospects

Generally, the excitation and emission wavelengths of lanthanide-based PLNPs are not correlated with the synthesis method. However, different synthesis methods can produce lanthanide-based PLNPs with significantly different crystallinity, defect density, particle size and morphology, which largely determines the luminescence intensity and quantum yield (QY) of the lanthanide-based PLNPs. The selection principle for the preparation of lanthanide-based PLNPs relies on the specific application area. For example, if bright persistent luminescence is needed for decoration or lighting, solid-state reactions are suggested since this method can produce

lanthanide-based PLNPs with strong emission intensity and high QY. The co-precipitation, hydrothermal method and thermal decomposition method can be used to synthesize PLNPs with a narrow particle size distribution, controllable morphology, good dispersibility and high crystallinity, which is suitable for biological applications such as bioimaging and cancer therapy. The available synthetic conditions may be another important consideration in selecting the synthesis method for practical application. For example, the hydrothermal and thermal decomposition methods require specific systems for satisfying the high-temperature reaction. Additionally, time efficiency is also important in the synthesis of PLNPs. The microwave-assisted synthesis is the most time-efficient among the described methods.

Although some achievements have been made in the development of lanthanide-based PLNPs, there are still several problems that need to be solved. Firstly, achieving highly bright and long-lasting persistent luminescence is still a challenge for lanthanide-based PLNPs. Persistent luminescence of PLNPs is highly dependent on the size, phase, trap density, trap level, energy transfer pathways, etc. These parameters need to be rationally designed for improving the persistent luminescence properties of lanthanide-based PLNPs. Secondly, most lanthanide-based PLNPs are charged by UV light, which seriously limits their biomedical applications since UV light possesses poor tissue penetration and may cause serious tissue damage. There is a strong need to design lanthanide-based PLNPs that can be charged by light sources with deep tissue penetration for reactivation of the persistent luminescence signal *in vivo*. Recently, the studies on X-ray charged PLNPs provide reliable methods for the reactivation of the persistent luminescence in deep tissues. Thirdly, the emission wavelength of lanthanide-based PLNPs is usually located in the visible or NIR-I region. The abundant energy levels of lanthanide ions can offer enormous energy-transfer pathways for realizing NIR-II/III persistent emissions, even NIR-I-to-NIR-II/III persistent luminescence. Last but not the least, lanthanide-based PLNPs with sizes smaller than 10 nm are necessary for clearance in biological systems. The synthesis of ultra-small PLNPs with bright persistent luminescence remains challenging. Advanced protocols for the synthesis of sub-10 nm lanthanide-based PLNPs by means including hetero-valence doping need to be explored in the future.

5. Conclusions

Lanthanide-based PLNPs are excellent luminescent materials with a broad emission range and ultra-long persistent decay due to the ladder-like energy structure of lanthanide ions and the abundant energy transfer pathways in the system. With the ongoing study toward the biomedical applications of lanthanide-based PLNPs in biomedicine, synthesis methods are in need to prepare lanthanide-based PLNPs with desired properties including size, surface functionalization, persistent luminescence intensity, emission wavelength, and decay time. In this review, we summarized several commonly used methods to prepare lanthanide-based PLNPs. The summarized methods such as the hydrothermal method and thermal decomposition method hold great promise in the controlled preparation of lanthanide-based PLNPs. Although some achievements have been made, there is still a strong need to enhance the brightness of the persistent luminescence after excitation ceases. Synthesis strategies that can fine-tune the crystal defects in lanthanide-based PLNPs need to be proposed to improve the persistent luminescence performance of PLNPs. In a word, the synthesis methods of lanthanide-based PLNPs are preliminarily mature and still stepping forward.

7. References

1. Matsuzawa T, Y Aoki, N Takeuchi, Y Murayama. A new long phosphorescent phosphor with high brightness, $SrAl_2O_4:Eu^{2+},Dy^{3+}$. J Electrochem Soc. 1996; 134(8): 2670.

2. Rojas-Hernandez RE, Rubio-Marcos F, Rodriguez MA, Fernandez JF. Long lasting phosphors: $SrAl_2O_4:Eu,Dy$ as the most studied material. Renewable Sustainable Energy Rev. 2018; 81(2): 2759.

3. Liang L, Chen N, Jia YY, Ma QQ, Wang J, Yuan Q, et al. Recent progress in engineering near-infrared persistent luminescence nanoprobes for time-resolved biosensing/bioimaging. Nano Res. 2019; 12(6): 1279.

4. Fritzen DL, Giordano L, Rodrigues LCV, Monteiro JHSK. Opportunities for persistent luminescent nanoparticles in luminescence imaging of biological systems and photodynamic therapy. Nanomaterials. 2020; 10(10): 2015.

5. Wang J, M QQ, Wang YQ, Shen HJ, Yuan Q. Recent progress in biomedical applications of persistent luminescence nanoparticles. Nanoscale. 2017; 9: 6204.

6. Wu, SQ, Li Y, Ding WH, Xu LT, Ma Y, Zhang LB. Recent advances of persistent luminescence nanoparticles in bioapplications. Nano-Micro Lett. 2020; 12(1): 70.

7. Su GM, Shen RC, Tan J, Yuan Q. Progress on the application of long persistent phosphors in photocatalytic system. Chemical Journal of Chinese Universities. 2020; 41(11): 2404.

8. Liu YS, Tu DT, Zhu HM, Chen XY. Lanthanide-doped luminescent nanoprobes: controlled synthesis, optical spectroscopy, and bioapplications. Chem Soc Rev. 2013; 42: 6924.

9. Zhang LW, Shen RC, Tan J, Yuan Q. Influence of doped ions on persistent luminescence materials: a review. Chin J Struct Chem. 2021; 2:148.

10. Sun LN, Wei RY, Feng J, Zhang HJ. Tailored lanthanide-doped upconversion nanoparticles and their promising bioapplication prospects. Coord Chem Rev. 2018; 364: 10.

11. Song YP, Lu MY, Mandl GA, Xie Y, Sun GT, Chen JB, et al. Energy Migration Control of Multimodal Emissions in an Er^{3+}-Doped Nanostructure for Information Encryption and Deep-Learning Decoding. Angew Chem Int Ed. 2021; 60: 23790.

12. Li XM, Zhang F, Zhao DY. Lab on upconversion nanoparticles: optical properties and applications engineering via designed nanostructure. Chem Soc Rev. 2015; 44(6): 1346.

13. Liu HY, Li JB, Hu PF, Sun SQ, Shi LY, Sun LN. Facile synthesis of Er^{3+}/Tm^{3+} co-doped magnetic/luminescent nanosystems for possible bioimaging and therapy applications. J Rare Earths. 2022; 40: 11.

14. Song L, Lin XH, Song XR, Chen S, Chen XF, Li J, et al. Repeatable deep-tissue activation of persistent luminescent nanoparticles by soft X-ray for high sensitivity long-term in vivo bioimaging. Nanoscale, 2017; 9: 2718.

15. Sun SK, Wang HF, Yan XP. Engineering persistent luminescence nanoparticles for biological applications: from biosensing/bioimaging to theranostics. Acc Chem Res. 2018; 51(5): 1131.

16. Ou XY, Qin X, Huang BL, Zan J, Wu QX, Hong ZZ, et al. High-resolution X-ray luminescence extension imaging. Nature. 2021; 590(7846): 410.

17. Lin QS, Li ZH, Yuan Q. Recent advances in autofluorescence-free biosensing and bioimaging based on persistent luminescence nanoparticles. Chin Chem Lett. 2019; 30(9): 1547.

18. Lin QS, Li ZH, Ji CH, Yuan Q. Electronic structure engineering and biomedical applications of low energy-excited persistent luminescence nanoparticles. Nanoscale Adv. 2020; 2(4): 1380.

19. Luo Q, Wang WJ, Tan J, Yuan Q. Surface modified persistent luminescence probes for biosensing and bioimaging: a review. Chin J Chem. 2021; 39(4): 1009.

20. Jia YY, Wang WJ, Liang L, Yuan Q. Bioassay applications of aptamer-functionalized rare earth nanomaterials. Acta Chim Sinica. 2020; 78(11): 1177.

21. Ma QQ, Wang J, Li ZH, Lv XB, Liang L, Yuan Q. Recent progress in time-resolved biosensing and bioimaging based on lanthanide-doped nanoparticles. Small. 2019; 15(32): 1804969.

22. Song HJ, Chen DH. Combustion synthesis and luminescence properties of $SrAl_2O_4$:Eu^{2+},Dy^{3+},Tb^{3+} phosphor. Luminescence. 2007; 22(6): 544.

23. Bierwagen J, Delgado T, Jiranek G, Yoon S, Gartmann N, Walfort B, et al. Probing traps in the persistent phosphor $SrAl_2O_4$:Eu^{2+},Dy^{3+},B^{3+}- A wavelength, temperature and sample dependent thermoluminescence investigation. J Lumin. 2020; 222: 117113.

24. Zhang HJ, Zhao X, Chen LJ, Yang CX, Yang XP. Study on optical properties of rare-earth ions in nanocrystalline monoclinic $SrAl_2O_4$:Ln (Ln = Ce^{3+}, Pr^{3+}, Tb^{3+}). J Phys Chem B. 2005; 109(30): 14396.

25. Tang MM, Wang XS, Peng DF, Wang W, Sun HQ, Yao X. Strong green and red up-conversion emission in Ho^{3+}, Yb^{3+} and Li^+ co- or tri-doped $SrAl_2O_4$ ceramics. J Alloys Compd. 2012; 529: 49.

26. Song K, Mo JG, Chen W, Feng K. Hydrothermal synthesis and luminescence of $SrAl_2O_4$:Eu^{2+}/Yb^{3+} hierarchical nanostructures. J Mater Sci: Mater Electron. 2016; 27(1): 49.

27. Xu YF, Ma DK, Guan ML, Chen XA, Pan QQ, Huang SM. Controlled synthesis of single-crystal $SrAl_2O_4$:Eu^{2+},Dy^{3+} nanosheets with long-lasting phosphorescence. J Alloys Compd. 2010; 502(1): 38.

28. Cheng BC, Zhang ZD, Han ZH, Xiao YH, Lei SJ. $SrAl_2O_4$:Eu^{2+},Dy^{3+} nanobelts: synthesis by combustion and properties of long-persistent phosphorescence. J Mater Res. 2011; 26(17): 2311.

29. Yu NY, Liu F, Li XF, Pan ZW. Near infrared long-persistent phosphorescence in $SrAl_2O_4$:Eu^{2+},Dy^{3+},Er^{3+} phosphors based on persistent energy transfer. Appl Phys Lett. 2009; 95(23): 231110.

30. Jia DD, Wang XJ, Jia W, Yen WM. Trapping processes of 5d electrons in Ce^{3+} doped $SrAl_2O_4$. J Lumin. 2007; 122: 311.

31. Li Z, Hao SS, Ji WW, Hao LY, Yin LJ, Xu X, Agathopoulos S. Mechanism of long afterglow in $SrAl_2O_4$:Eu phosphors. Ceram Int. 2021; 47(23): 32947.

32. Teng Y, Zhou JJ, Khisro SN, Zhou SF, Qiu JR. Persistent luminescence of $SrAl_2O_4$:Eu^{2+},Dy^{3+},Cr^{3+} phosphors in the tissue transparency window. Mater Chem Phys. 2014; 147(3): 772.

33. Xie QD, Li BW, He X, Zhang M, Chen Y, Zeng QQ. Correlation of structure, tunable colors, and lifetimes of (Sr, Ca, Ba)Al_2O_4:Eu^{2+},Dy^{3+} phosphors. Materials. 2017; 10(10): 1198.

34. Chen WB, Wang YH, Zeng W, Li G, Guo HJ. Design, synthesis and characterization of near-infrared long persistent phosphors $Ca_4(PO_4)_2O:Eu^{2+},R^{3+}$ (R = Lu, La, Gd, Ce, Tm, Y). RSC Adv. 2016; 6(1): 331.

35. Wiglusz RJ, Grzyb T, Bednarkiewicz A, Lis S, Strek W. Investigation of structure, morphology, and luminescence properties in blue-red emitter, europium-activated $ZnAl_2O_4$ nanospinels. Eur J Inorg Chem. 2012; 21: 3418.

36. Qu XF, Cao LX, Liu W, Su G, Wang PP, Schultz I. Sol-gel synthesis of long-lasting phosphors $CdSiO_3:Mn^{2+},RE^{3+}$ (RE = Tb, Eu, Nd) and luminescence mechanism. Mater Res Bull. 2012; 47(6): 1598.

37. Jun GF, Hu YH, Chen L, Yang ZF, Wang T, Jin YH, et al. Effects of Ln^{3+} (Ln=Ce, Pr, Tb and Lu) doping on the persistent luminescence properties $BaMg_2(PO_4)_2:Eu^{2+}$ phosphor. Ceram Int. 2015; 41(10): 14998.

38. Kumar K, Singh AK, SB Rai. Laser excited long lasting luminescence in $CaAl_2O_4:Eu^{3+}/Eu^{2+} + Nd^{3+}$ phosphor. Spectrochim Acta Part A. 2013; 102: 212.

39. Tian YM, Zhang P, Zheng ZT, Chai YS. A novel approach for preparation of $Sr_3Al_2O_6:Eu^{2+},$ Dy^{3+} nanoparticles by sol–gel–microwave processing. Mater Lett. 2012; 73:157.

40. Wan MH, Wang YH, Wang XS, Zhao H, Li HL Wang C. Long afterglow properties of Eu^{2+}/Mn^{2+} doped Zn_2GeO_4. J Lumin. 2014; 145: 914.

41. Maldiney T, Lecointre A, Viana B, Bessiere A, Bessodes M, Gourier D, et al. Controlling electron trap depth to enhance optical properties of persistent luminescence nanoparticles for in vivo imaging. J Am Chem Soc. 2011; 133(30): 11810.

42. Rodriguez BDC, Sharma SK, Dorenbos P, Viana B, Capobianco JA. Persistent and photostimulated red emission in $CaS:Eu^{2+},Dy^{3+}$ nanophosphors. Adv Opt Mater. 2014; 34: 551.

43. Wang ZZ, Song Z, Ning LX, Xia ZG, Liu QL. Enhanced yellow persistent luminescence in $Sr_3SiO_5:Eu^{2+}$ through Ge Incorporation. Inorg Chem. 2019; 58(13): 8693.

44. Ju GF, Hu YH, Chen L, Wang XJ, Mu ZF. Recent progress in Eu^{2+}-activated phosphate persistent phosphors. Opt Mater. 2014; 36(11): 1920.

45. Van den Eeckhout K, Smet PF, Poelman D. Persistent Luminescence in Eu^{2+}-Doped Compounds: A Review. Materials. 2010; 3(4): 2536.

46. Van den Eeckhout K, Poelman D, Smet PF. Persistent Luminescence in Non-Eu^{2+}-Doped Compounds: A Review. Materials. 2013; 6(7): 2789.

47. Gao Y, Li R, Zheng W, Shang X, Wei J, Zhang M, et al. Broadband NIR photostimulated luminescence nanoprobes based on $CaS:Eu^{2+},Sm^{3+}$ nanocrystals. Chem Sci. 2019; 10: 5452.

48. Poelman D, Van der Heggen D, Du J, Cosaert E, Smet PF. Persistent phosphors for the future: Fit for the right application. J Appl Phys. 2020, 128: 240903.

49. Nimmegeers B, Cosaert E, Carbonati T, Meroni D, Poelman D. Synthesis and characterization of $GdVO_4:Nd$ near-infrared phosphors for optical time-gated in vivo imaging. Mater. 2020; 13(16): 3564.

50. Walfort B, Gartmann N, Afshani J, Rosspeintner A, Hagemann H. Effect of excitation wavelength (blue vs near UV) and dopant concentrations on afterglow and fast decay of persistent phosphor $SrAl_2O_4:Eu^{2+},Dy^{3+}$. J Rare Earths. 2021; DOI: 10.1016/j.jre.2021.07.014.

51. Wu MH, Chen W, Liu SY, Sun YC, Huang LF, Chen GL, et al. Sensitizing effect of Nd^{3+} on Tb^{3+} activated ZrP_2O_7 long persistent phosphor materials. J Rare Earths. 2021; 39(7): 757.

52. Zhang H, Yang Z, Zhao L, Cao JY, Yu X, Yang Y, et al. Long persistent luminescence from all-Inorganic perovskite nanocrystals. Adv Opt Mater. 2020; 8(18): 2000585.

53. Ji CL, Tan J, Yuan Q. Defect Luminescence based persistent phosphors—from controlled synthesis to bioapplications. Chin J Chem. 2021; 39(12): 3188.

54. Xi J, Chen N, Yang YB, Yuan Q. Recent progress in controlled synthesis of persistent luminescence nanomaterials for diagnosis applications. Chemical Journal of Chinese University.2021; 42(11): 3247.

55. Xu J, Murata D, Ueda J, Tanabe S. Near-infrared long persistent luminescence of Er^{3+} in garnet for the third bio-imaging window. J Mater Chem C. 2016; 4(47): 11096.

56. Liang YJ, Liu F, Chen YF, Wang XL, Sun KN, Pan ZW. Red/near-infrared/short-wave infrared multi-band persistent luminescence in Pr^{3+}-doped persistent phosphors. Dalton Trans. 2017; 46(34): 11149.

57. Cai YY, Liu BT, Chen WB, Qiu JB, Xu XH, Zhao L, et al. X-ray and UV excited long persistent luminescence properties of $Zn_3Ga_2GeO_8$:Cr^{3+},Pr^{3+}. ECS J Solid State Sci Technol. 2020; 9(6): 066006.

58. Rusu E, Ursaki V, Novitschi G, Vasile M, Petrenco P, Kulyuk L. Luminescence properties of $ZnGa_2O_4$ and $ZnAl_2O_4$ spinels doped with Eu^{3+} and Tb^{3+} ions. Phys Status Solidi C. 2009; 6(5): 1199.

59. Wang N, Li TJ, Han LL, Wang YC, Ci ZP, Wang YH, et al. The fluorescence self-healing mechanism and temperature-sensitive properties of a multifunctional phosphosilicate phosphor. J Mater Sci. 2019; 54: 6434.

60. Zhang HJ, Zhao X, Chen LJ, Yang CX, Yuan XP. Dendrimer grafted persistent luminescent nanoplatform for aptamer guided tumor imaging and acid-responsive drug delivery. Talanta. 2020; 219: 121209.

61. Sengar P, Hirata GA, Farias MH, Castillón F. Morphological optimization and (3-aminopropyl) trimethoxy silane surface modification of $Y_3Al_5O_{12}$:Pr nanoscintillator for biomedical applications. Mater Res Bull. 2016; 77: 236.

62. Bonturim E, Merízio LG, Dos Reis R, Brito HF, Rodrigues LCV, Felinto MCFC. Persistent luminescence of inorganic nanophosphors prepared by wet-chemical synthesis. J Alloys Compd. 2018; 732(25): 705.

63. Homayoni H, Ma L, Zhang JY, Sahi SK, Rashidi LH, Bui B, et al. Synthesis and conjugation of $Sr_2MgSi_2O_7$:Eu^{2+},Dy^{3+} water soluble afterglow nanoparticles for photodynamic activation. Photodiagn Photodyn Ther. 2016; 16: 90.

64. Homayoni H, Ma L, Zhang JY, Sahi SK, Rashidi LH, Bui B, et al. Study on the persistent luminescence of diopside nanotracers $CaMgSi_2O_6$:Eu^{2+},Mn^{2+},Pr^{3+}. Proc SPIE. 2016; 9749: 97490.

65. Duan XX, Huang SH, You FT, Xu Z, Teng F, Yi LX, et al. Electrooptical characteristics of nanoscale and bulk long persistent phosphor $SrAl_2O_4$:Eu,Dy. J Exp Nanosci. 2009; 4(2): 169.

66. Tabanli S, Yilmaz HC, Bilir G, Erdem M, Eryurek G, Di Bartolo B, et al. Broadband, white light emission from doped and undoped insulators. ECS J Solid State Sci Technol. 2018; 7(1): R3199.

67. Wiglusz RJ, Grzyb T, Bednarkiewicz A, Lis S, Strek W. Investigation of structure, morphology, and luminescence properties in blue-red emitter, europium-activated $ZnAl_2O_4$ nanospinels. Eur J Inorg Chem. 2021; 21: 3418.

68. Niioka H, Yamasaki J, Dung DTK, Miyake J. Enhancement of near-infrared luminescence of Y_2O_3:Ln,Yb (Ln = Tm, Ho, Er) by Li-ion doping for cellular bioimaging. Chem Lett. 2016; 45: 1406.

69. Danks AE, Hall SR, Schnepp Z. The evolution of 'sol–gel' chemistry as a technique for materials synthesis. Mater Horiz. 2016; 3(2): 91.

70. Li N, Li YH, Han YY, Pan W, Zhang TT, Tang B. A highly selective and instantaneous nanoprobe for detection and imaging of ascorbic acid in living cells and in vivo. Anal Chem. 2014; 86(8): 3924.

71. He XW, Liu XF, Li RF, Yang B, Yu KL, Zeng M, et al. Effects of local structure of Ce^{3+} ions on luminescent properties of $Y_3Al_5O_{12}$:Ce nanoparticles. Sci Rep. 2016; 6: 22238.

72. Fabitha K, Rao MSR. Ho^{3+}-doped ZnO nano phosphor for low-threshold sharp red light emission at elevated temperatures. J Opt Soc Am B. 2017; 34(12): 2485.

73. Khamehchi FASA, Winarski D, Agarwal S. Synthesis and characterization of Ce:YAG nano phosphors and ceramics. Opt Mater Express. 2016; 6(12): 3704.

74. Manali IF, Rodrigues LCV, Braga AH, Galante D, Teixeira VC. Structural and optical properties of europium- and titanium doped Y_2O_3 nanoparticles. Luminescence. 2020; 35(4): 456.

75. Abdukayum A, Chen JT, Zhao Q, Yan XP. Functional near infrared-emitting Cr^{3+}/Pr^{3+} Co-doped zinc gallogermanate persistent luminescent nanoparticles with superlong afterglow for in vivo targeted bioimaging. J Am Chem Soc. 2013; 135(38): 14125.

76. Hu XW, Yang H, Guo TT, Shu DH, Shan, WF, Li, GZ, et al. Preparation and properties of Eu and Dy co-doped strontium aluminate long afterglow nanomaterials. Ceram Int. 2018; 44(7): 7535.

77. Yang HJ, Yuan L, Zhu GS, Yu AB, Xu HR. Luminescent properties of YAG:Ce^{3+} phosphor powders prepared by hydrothermal-homogeneous precipitation method. Mater Lett. 2009; 63(27): 2271.

78. Ma QQ, Wang J, Zheng W, Wang Q, Li ZH, Yuan Q, et al. Controlling disorder in host lattice by hetero-valence ion doping to manipulate luminescence in spinel solid solution phosphors. Sci China Chem. 2018; 61(12): 1624.

79. Huo QY, Tu WX, Guo L. Enhanced photoluminescence property and broad color emission of $ZnGa_2O_4$ phosphor due to the synergistic role of Eu^{3+} and carbon dots. Opt Mater. 2017; 72: 305.

80. Dai WB, Lei YF, Zhou J, Xu M, Chu LL, Li L. Near-infrared quantum-cutting and long-persistent phosphor $Ca_3Ga_2Ge_3O_{12}$:Pr^{3+},Yb^{3+} for application in in vivo bioimaging and dye-sensitized solar cells. J Alloys Compd. 2017; 726(5): 230.

81. Liu D, Cui C, Huang P, Wang L, Jiang GW. Luminescent properties of red long-lasting phosphor Y_2O_2S:Eu^{3+},M^{2+} (M = Mg, Ca, Sr, Ba), Ti^{4+} nanotubes via hydrothermal method. J Alloys Compd. 2014; 583(15): 530.

82. Srivastava BB, Gupta SK, Barbosa R, Villarreal A, Lozano K, Mao YB. Rare earth free bright and persistent white light emitting zinc gallo-germanate nanosheets: technological advancement to fibers with enhanced quantum efficiency. Mater Adv. 2021; 2: 4058.

83. Li ZJ, Zhang YW, Wu X, Huang L, Li DS, Fan W, et al. Direct aqueous-phase synthesis of sub-10 nm "Luminous Pearls" with enhanced in vivo renewable near-infrared persistent luminescence. J Am Chem Soc. 2015; 137(16): 5304.
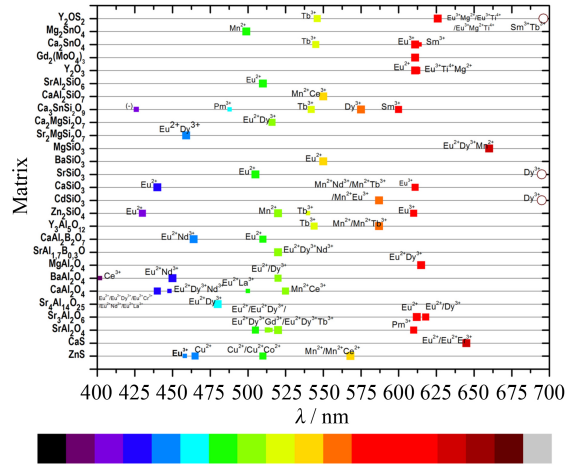
84. Yang J, Jiang RY, Meng YQ, Zhao YY, Wang MW, Zhu HC, et al. NIR-I/III afterglow induced by energy transfers between Er and Cr codoped in ZGGO nanoparticles for potential bioimaging. J Am Ceram Soc. 2021; 104: 4637.

85. Caratto V, Locardi F, Costa GA, Masini R, Fasoli M, Panzeri L, et al. NIR persistent luminescence of lanthanide ion-doped rare-earth oxycarbonates: the effect of dopants. ACS Appl Mater Interfaces. 2014; 6(20): 17346.

86. Liu XW, Ji Q, Hu QY, Li C, Chen ML, Sun J, et al. Dual-mode long-lived luminescence of Mn^{2+}-doped nanoparticles for multilevel anticounterfeiting. ACS Appl Mater Interfaces. 2019; 11(33): 30146.

87. Pei P, Chen Y, Sun CX, Fan Y, Yang YM, Liu X, et al. X-ray-activated persistent luminescence nanomaterials for NIR-II imaging. Nat. Nanotechnol. 2021; 16(9): 1011.

88. Huang K, Li ZJ, Li Y, Yu N, Gao XP, Huang L, et al. Three-dimensional colloidal controlled growth of core–shell heterostructured persistent luminescence nanocrystals. Nano Lett. 2021; 21(12): 4903.

89. Lv XB, Chen N, Wang J, Yuan Q. Facile thermal decomposition synthesis of sub-5 nm nanodots with long-lived luminescence for autofluorescence-free bioimaging. Sci China Mater. 2020; 63(9): 1808.

90. Kumar V, Pitale SS, Mishra V, Nagpure IM, Biggs MM, Ntwaeaborwa OM, et al. Luminescence investigations of Ce^{3+} doped CaS nanophosphors. J Alloys Compd. 2010; 492(1-2): L8.

91. Xue ZP, Deng SQ, Liu YL, Lei BF, Xiao Y, Zheng MT. Synthesis and luminescence properties of $SrAl_2O_4$:Eu^{2+},Dy^{3+} hollow microspheres via a solvothermal co-precipitation method. J Rare Earths. 2013; 31(3): 241.

92. Zheng W, Zhou SY, Chen Z, Hu P, Liu YS, Tu DT, et al. Sub-10 nm lanthanide-doped CaF_2 nanoprobes for time-resolved luminescent biodetection. Angew Chem Int Ed. 2013; 52 (26): 6671.

93. Ou XY, Chen YY, Xie LL, Chen J, Zan J, Chen XF, et al. X-ray nanocrystal scintillator-based aptasensor for autofluorescence-free detection. Anal Chem. 2019; 91(15): 10149.

94. Cheng BC, Liu HJ, Fang M, Xiao YH, Lei SJ, Zhang LD. Long-persistent phosphorescent $SrAl_2O_4$:Eu^{2+},Dy^{3+} nanotubes. Chem. Commun. 2009; 8: 944.

95. Xu XJ, Sun XD, Liu H, Li JG, Li XD, Huo D, Liu S. Synthesis of monodispersed spherical yttrium aluminum garnet (YAG) powders by a homogeneous precipitation method. J Am Ceram Soc. 2018; 95(12): 3821.

96. Ju GF, Hu YH, Chen L, Jin YH, Li Y. Persistent luminescence in $BaGd_2O_4$:Dy^{3+}: from blue to infrared. Appl Phys A. 2018; 124: 39.

97. Qin HM, Liu H, Sang YH, Lv YH, Zhang XL, Zhang YY, et al. Ammonium sulfate regulation of morphology of Nd:Y_2O_3 precursor via urea precipitation method and its effect on the sintering properties of Nd:Y_2O_3 nanopowders. Cryst Eng Comm. 2012; 14(5): 1783.

98. Song L, Dong Y, Shao QY, Jiang JQ. Preparation of $Y_3Al_5O_{12}$: Ce nanophosphors using salt microemulsion method and their luminescent properties. J Mater Sci. 2018; 53(21):15196.

99. Li ZJ, Zhang HW, Fu HX. Facile synthesis and morphology control of Zn_2SiO_4:Mn nanophosphors using mesoporous silica nanoparticles as templates. J Lumin. 2013; 135: 79.

100. Li ZJ, Zhang YJ, Zhang HW, Fu HX. Long-lasting phosphorescence functionalization of mesoporous silica nanospheres by $CaTiO_3$:Pr^{3+} for drug delivery. Microporous Mesoporous Mater. 2013; 176: 48.

101. Li ZJ, Zhang HW, Sun M, Shen JS, Fu HX. A facile and effective method to prepare long-persistent phosphorescent nanospheres and its potential application for in vivo imaging. J Mater Chem. 2012; 22: 24713.

102. Xin SY, Wang YH, Dong PY, Zeng W, Zhang J. Preparation, characterization, and luminescent properties of $CaAl_2O_4$:Eu^{2+},Nd^{3+} nanofibers using core–sheath $CaAl_2O_4$:Eu^{2+},Nd^{3+} carbon nanofibers as templates. J Mater Chem C. 2013; 1: 8156.

103. Xu ZK, Duan GT, Zhang HW, Wang YY, Xu L, Cai WP. In situ synthesis of porous array films on a filament induced micro-gap electrode pair and their use as resistance-type gas sensors with enhanced performances. Nanoscale. 2015; 7: 14264.

104. Li ZJ, Shi, JP, Zhang HW, Sun M. Highly controllable synthesis of near-infrared persistent luminescence SiO_2/$CaMgSi_2O_6$ composite nanospheres for imaging *in vivo.* Opt Express. 2014; 22: 10509.

105. Egodawatte S, Zhang E, Posey TJ, Gimblet GR, Foulger SH, zur Loye HC. Synthesis of scintillating Ce^{3+}-doped $Lu_2Si_2O_7$ nanoparticles using the salt-supported high temperature (SSHT) method: solid state chemistry at the nanoscale. ACS Appl Nano Mater. 2019; 2(4): 1857.

106. Shi TH, Sun WJ, Qin RX, Li DS, Feng YS, Chen L, et al. X-Ray-induced persistent luminescence promotes ultrasensitive imaging and effective inhibition of orthotopic hepatic tumors. Adv Funct Mater. 2020; 30(24): 2001166.

107. Zou R, Gao YF, Zhang Y, Jiao J, Wong KL, Wang J. ^{68}Ga-labeled magnetic-NIR persistent luminescent hybrid mesoporous nanoparticles for multimodal imaging-guided chemotherapy and photodynamic therapy. ACS Appl Mater Interfaces. 2021; 13(8): 9667.

108. Vaidhyanathan B, Binner JGP. Microwave assisted synthesis of nanocrystalline YAG. J Mater Sci. 2006; 41(18): 5954.

109. Molefe FV, Noto LL, Dhlamini MS, Mothudi BM, Orante-Barron, VR. Structural, photoluminescence and thermoluminescence study of novel Li^+ co-activated lanthanum oxide activated with Dy^{3+} and Eu^{3+} obtained by microwave-assisted solution combustion synthesis. Opt Mater. 2019; 88: 540.

110. Jain A, González CAE, Tejeda EM, Durán A, Contreras OE, Hirata GA. Covering the optical spectrum through different rare-earth ion-doping of YAG nanospheres produced by rapid microwave synthesis. Ceram Int. 2018; 44(2): 1886.

111. Pedroso CCS, Carvalho JM, Rodrigues LCV, Holsa, J, Brito HF. Rapid and energy-saving microwave-assisted solid-state synthesis of Pr^{3+}-, Eu^{3+}-, or Tb^{3+}-doped Lu_2O_3 persistent luminescence materials. ACS Appl Mater Interfaces. 2016; 80(5): 19593.

112. Hebbar, ND, Choudhari, KS, Pathak N, Shivashankar SA, Kulkarni SD. $ZnGa_{2-x}Eu_xO_4$ nanoparticles: 10 minutes microwave synthesis, thermal tuning of Eu^{3+} site distribution and photophysical properties. J Alloys Compd. 2018; 768: 676.

113. Qiu ZF, Zhou YY, Lu MK, Zhang AY, Ma Q. Combustion synthesis of long-persistent luminescent MAl_2O_4: Eu^{2+},R^{3+} (M = Sr, Ba, Ca, R = Dy, Nd and La) nanoparticles and luminescence mechanism research. Acta Mater. 2007; 55: 2615.

114. Xu YC, Chen DH. Combustion synthesis and photoluminescence of $Sr_2MgSi_2O_7$: Eu,Dy long lasting phosphor nanoparticles. Ceram Int. 2008; 34(8): 2117.

115. Jung JY, Hirata GA, Gundiah G, Derenzo S, Wrasidlo W, Kesari S, et al. Identification and development of nanoscintillators for biotechnology applications. J Lumin. 2014; 154: 569.
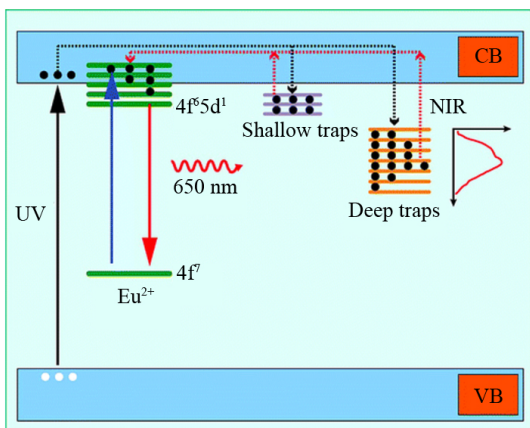
116. Jiang HM, Liu L, Yu KX, Yin XG, Zheng SH, Song L, et al. Cr^{3+}/Y^{3+} co-doped persistent luminescence nanoparticles with biological window activation for in vivo repeatable imaging. J Rare Earths. 2021; DOI：10.1016/j.jre.2021.05.007.

117. Can-Uc B, Montes-Frausto JB, Juarez-Moreno K, Licea-Rodriguez J, Rocha-Mendoza Israel, Hirata GA. Light sheet microscopy and $SrAl_2O_4$ nanoparticles codoped with Eu^{2+}/Dy^{3+} ions for cancer cell tagging. J Biophotonics. 2018; 11(6): e201700301.

118. Sanad MMS, Rayan DA, Rashad MM. Optical and photoluminesce properties of Eu^{2+}-activated strontium magnesium silicate phosphors using different rare-earth co-activators. Opt Quantum Electron. 2019; 51: 192.

119. Wu LY, Hu J, Zou QL, Lin YL, Huang DC, Chen DJ, et al. Synthesis and optical properties of a $Y_3(Al/Ga)_5O_{12}$: Ce^{3+},Cr^{3+},Nd^{3+} persistent luminescence nanophosphor: a promising near-infrared-II nanoprobe for biological applications. Nanoscale. 2020; 12: 14180.

120. Rojas-Hernandez RE, Rubio-Marcos F, Serrano A, Salas E, Hussainova I, Fernandez JF. Towards blue long-lasting luminescence of Eu/Nd-doped calcium-aluminate nanostructured platelets via the molten salt route. Nanomaterials. 2019; 9(10): 1473.

121. Cheng YL, Zhao Y, Zhang YF, Cao XQ. Preparation of $SrAl_2O_4:Eu^{2+},Dy^{3+}$ fibers by electrospinning combined with sol-gel process. J Colloid Interface Sci. 2010; 344(2): 321.

122. Yang YG, Liu B, Zhang YY, Lv XS, Wei L, Wang XP. Fabrication and luminescence of $BiPO_4:Tb^{3+}/Ce^{3+}$ nanofibers by electrospinning. Superlattices Microstruct. 2016; 90: 227.

123. Xue ZP, Deng SQ, Liu YL. Synthesis and luminescence properties of $SrAl_2O_4:Eu^{3+},Dy^{3+}$ nanosheets. Physica B Condensed Matter. 2012; 407(18): 3808.

124. Kong JT, Zheng W, Liu YS, Li RF, Ma E, Zhu HM, et al. Persistent luminescence from Eu^{3+} in SnO_2 nanoparticles. Nanoscale. 2015; 7(25): 11048.

125. Du HL, Castaing V, Guo DC, Viana B. Rare-earths doped-nanoparticles prepared by pulsed laser ablation in liquids. Ceram Int. 2020; 46(16): 26299.

126. Maldiney T, Sraiki G, Viana B, Gourier D, Richard C, Scherman DT, et al. *In vivo* optical imaging with rare earth doped $Ca_2Si_5N_8$ persistent luminescence nanoparticles. Opt Mater Express. 2012; 2(3): 261.

127. Sato K, Komuro S, Morikawa T, Aizawa H, Katsumata T, Harako S, et al. Long afterglow characteristics of thin film phosphor fabricated by laser ablation. J Cryst Growth. 2005; 275(1-2): 1137.

128. Du HL, Castaing V, Guo DC, Viana B. Rare-earths doped-nanoparticles prepared by pulsed laser ablation in liquids. Ceram Int. 2020; 46(16): 26299.

129. Huczko A, Kurcz M, Baranowski P, Bystrzejewski M, Bhattarai A, Dyjak S, et al. Fast combustion synthesis and characterization of $YAG:Ce^{3+}$ garnet nanopowders. Phys Status Solidi B. 2013; 250(12): 2702.

130. Singh D, Tanwar V, Samantilleke AP, Mari B, Bhagwan S, Singh KC, et al. Synthesis of $Sr_{(1-x-y)}Al_4O_7:Eu_x^{2+},Ln_y^{3+}$ (Ln = Dy, Y, Pr) nanophosphors using rapid gel combustion process and their down conversion characteristics. Electron Mater Lett. 2017; 13: 222.
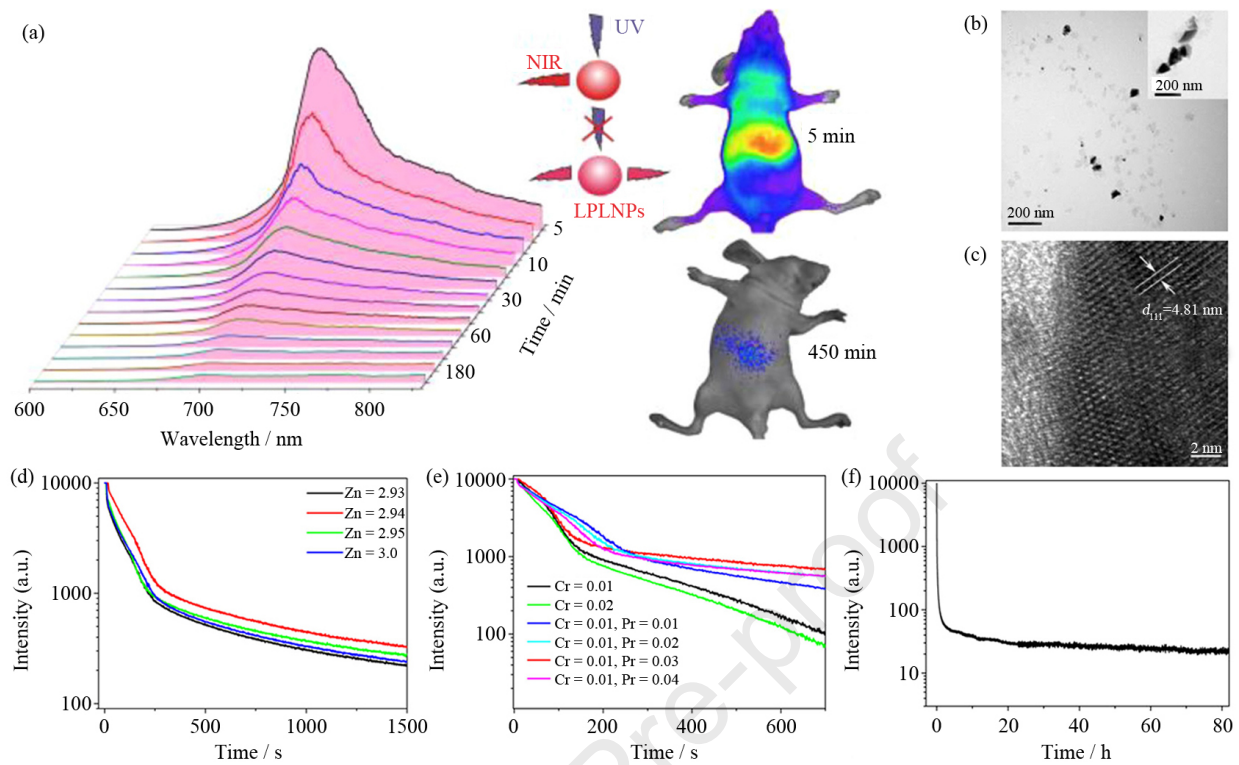
Graphical abstract:

This review summarizes the latest developments in the design and preparation of lanthanide-based persistent luminescence nanoparticles and discusses their prospects in biomedicine applications.
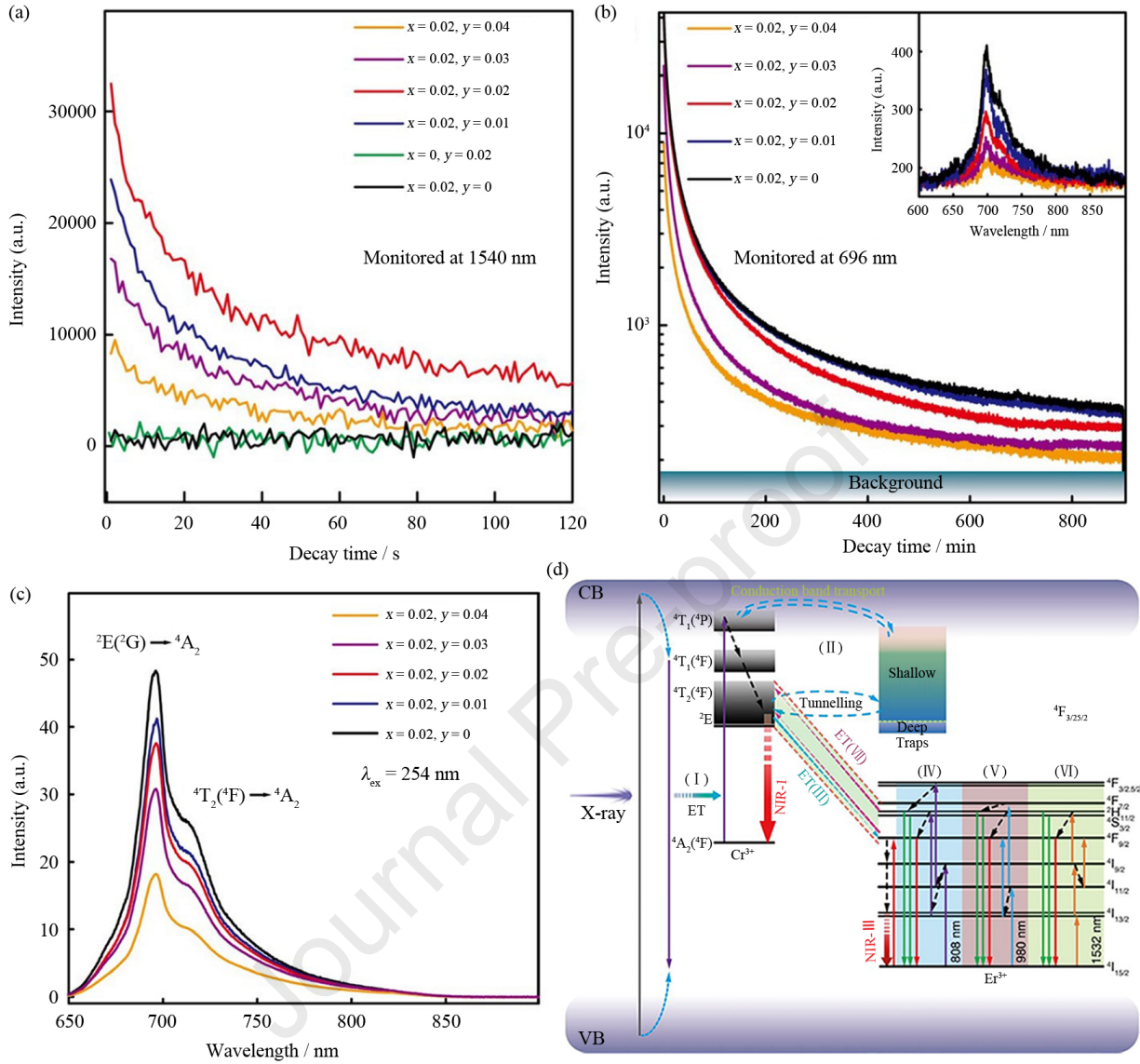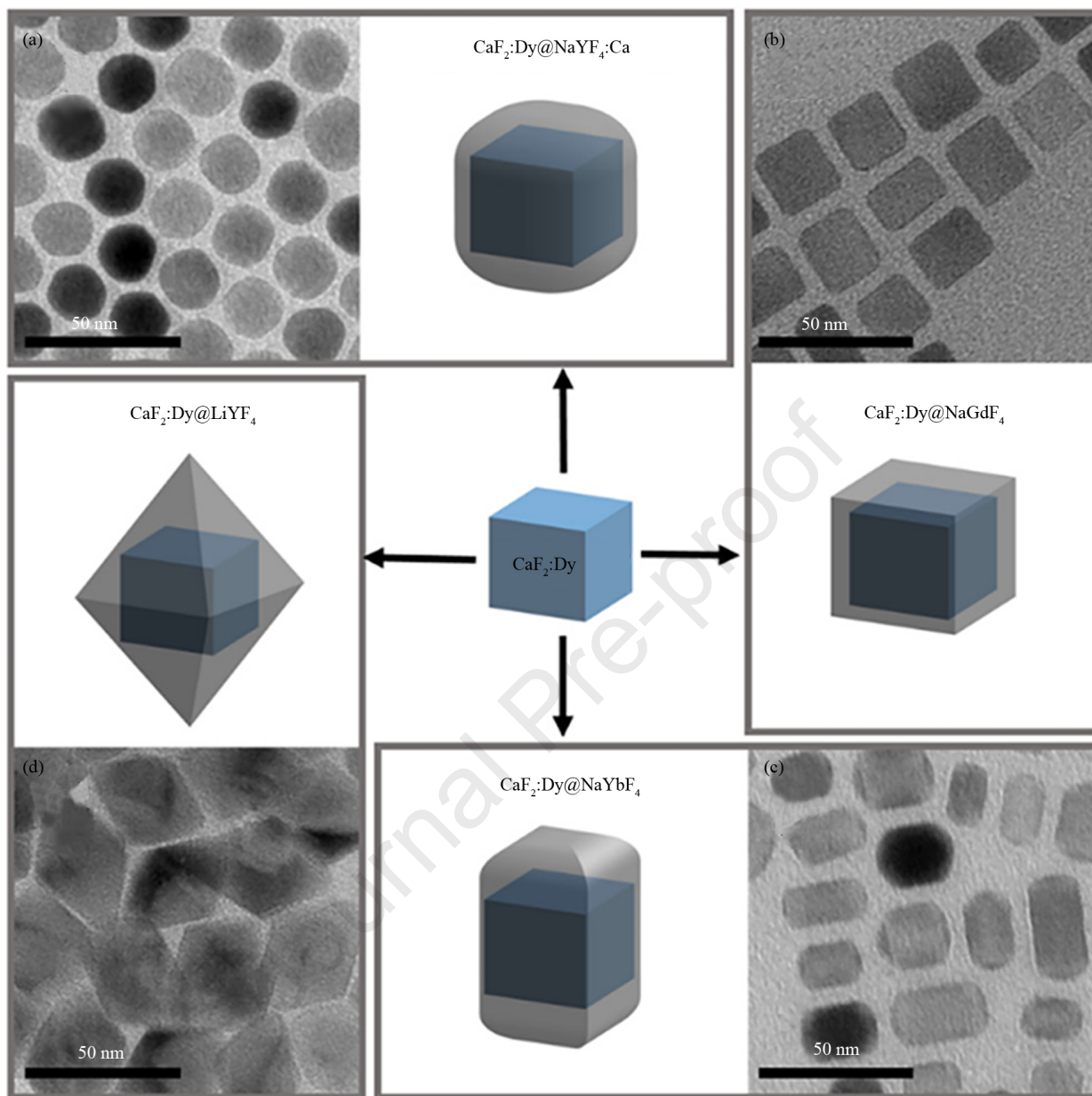
(a)

(b)

(c)

(d)

(e)

(f)

(a) Monitored at 1540 nm

x = 0.02, y = 0.04
x = 0.02, y = 0.03
x = 0.02, y = 0.02
x = 0.02, y = 0.01
x = 0, y = 0.02
x = 0.02, y = 0

(b) Monitored at 696 nm

x = 0.02, y = 0.04
x = 0.02, y = 0.03
x = 0.02, y = 0.02
x = 0.02, y = 0.01
x = 0.02, y = 0

Background

(c) $^2E(^2G) \longrightarrow {}^4A_2$

$^4T_2(^4F) \longrightarrow {}^4A_2$

λ_{ex} = 254 nm

x = 0.02, y = 0.04
x = 0.02, y = 0.03
x = 0.02, y = 0.02
x = 0.02, y = 0.01
x = 0.02, y = 0

(d)

(a) mZGGOs
200 nm

(b) mZGGOs
20 nm
5 nm

(c)
Adsorption
Desorption
S_{BET} = 18.4903 m^2/g
Adsorption volume (cm^3/g)
Relative pressure (p/p_0)

(d) mZGGOs
20 nm
Zn
Ga
Ge
Yb
Er
Cr

(e)
ZGGOs
mSiO$_2$
mZGGOs
ZnGa$_2$O$_4$ JCPDS NO.38-1240
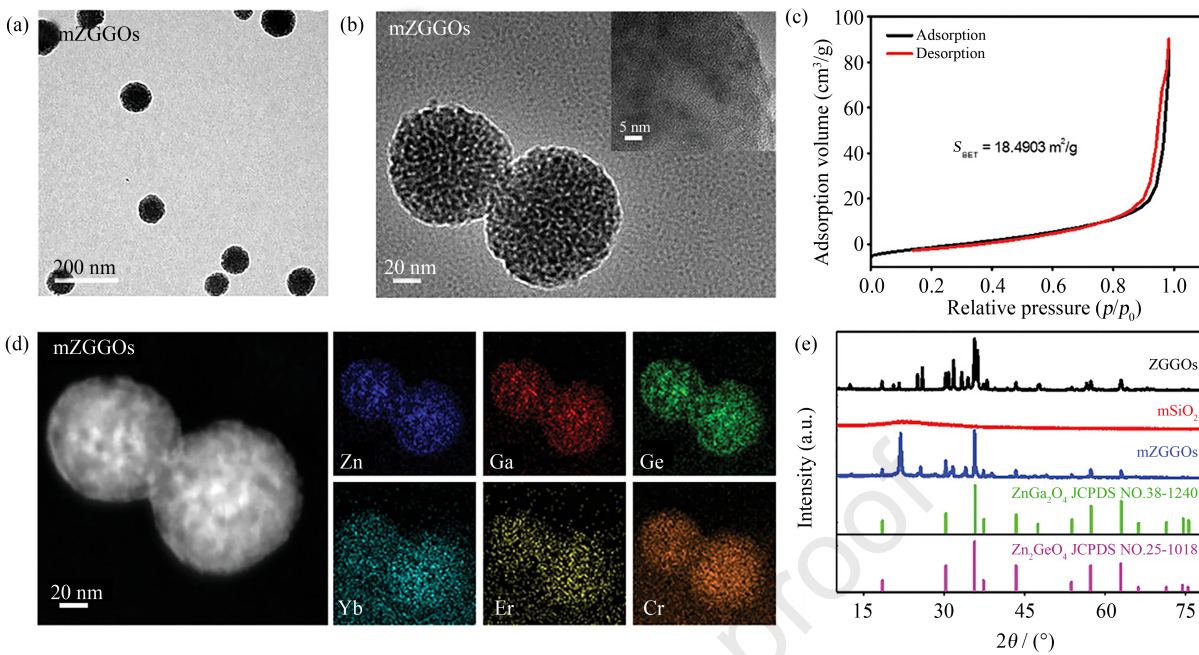Zn$_2$GeO$_4$ JCPDS NO.25-1018
Intensity (a.u.)
2θ / (°)

Declaration of interests

☒ The authors declare that they have no known competing financial interests or personal relationships that could have appeared to influence the work reported in this paper.

☐The authors declare the following financial interests/personal relationships which may be considered as potential competing interests: